Virchows Arch (2006) 448: 428–434
DOI 10.1007/s00428-005-0120-2

ORIGINAL ARTICLE

Phyu Phyu Aung · Yoshitsugu Mitani ·
Yuichi Sanada · Hirofumi Nakayama ·
Keisuke Matsusaki · Wataru Yasui

Differential expression of claudin-2 in normal human tissues and gastrointestinal carcinomas

Received: 3 October 2005 / Accepted: 10 October 2005 / Published online: 17 November 2005

Abstract Claudins are involved in the formation of tight junctions in epithelial and endothelial cells. Claudins form a family of 24 members displaying organ- and tissue-specific patterns of expression. In the present study, we evaluated the specificity of the claudin-2 expression in various normal human tissues and gastrointestinal cancers by quantitative reverse transcriptase–polymerase chain reaction and immunohistochemistry. In 14 various normal tissues, *claudin-2* mRNA was expressed in the kidney, liver, pancreas, stomach, and small intestine; the highest level of which was detected in the kidney. Colorectal cancers (CRCs) expressed *claudin-2* mRNA at high levels. Immunohistochemical analysis of claudin-2 in 146 gastric cancers (GCs) and 99 CRCs demonstrated claudin-2 expression in 2.1% of GCs and 25.3% of CRCs, respectively. There was no obvious correlation between claudin-2 expression and clinicopathological parameters of CRCs. These results suggest that the expression of claudin-2 may involve organ specificity, and increased expression of claudin-2 may participate in colorectal carcinogenesis.

Keywords Claudin-2 · Gastric · Colorectal cancers

P. P. Aung · Y. Mitani ·
Y. Sanada · H. Nakayama · W. Yasui (✉)
Department of Molecular Pathology,
Graduate School of Biomedical Sciences,
Hiroshima University,
1-2-3 Kasumi, Minami-ku,
Hiroshima 734-8551, Japan
e-mail: wyasui@hiroshima-u.ac.jp
Tel.: +81-82-2575145
Fax: +81-82-2575149

K. Matsusaki
Department of Surgery,
Hofu Institute of Gastroenterology,
14-33 Ekiminami, Hofu,
Yamaguchi 747-0801, Japan

Introduction

Claudin-1 and claudin-2 were the first members of the transmembrane tetraspan family of proteins identified as being involved in tight junction formation with the reruitment of occludin [4] and binding to other tight junction constituents [8]. Claudins form a family of at least 24 members displaying organ- and tissue-specific patterns of expression [9, 17]. Among the claudin family members, expression of claudin-2 is found in the liver, pancreas, and gut in normal rat tissues [17]. Claudin-2 expression is ubiquitous in the epithelial cells at the crypts of the small intestine but restricted to the undifferentiated cell compartment of the colon in rats [17]. Claudin-2 is also known to be expressed in mouse nephron [3, 9]. However, the expression pattern of claudin-2 remains to be elucidated in normal human tissues.

Gastrointestinal cancers including gastric cancer (GC) and colorectal cancer (CRC) are the most common malignancies worldwide. A better knowledge of changes in gene expression during gastrointestinal carcinogenesis may lead to new paradigms and possible improvements in diagnosis, treatment, and prevention. On the other hand, relatively little is known about the expression of claudins in human tumors, and only little information is available on the influence of claudin expression on tumor behavior. It was reported that the expression of claudin-7 was decreased in high-grade breast cancer [10]. Overexpression of claudin-4 has been found in pancreatic adenocarcinoma and its precursor lesions [15, 22], while overexpression of claudin-3 and claudin-4 has been found in prostate and ovarian carcinomas [7, 13]. Concerning the expression of claudin-2 in tumor tissue, it has been reported that claudin-2 expression was detected in 98 (52%) of 188 breast carcinomas [20]. There is one report showing claudin-2 expression in gastrointestinal tumors, but the sample number was small [21].

In the present study, the expression of claudin-2 was investigated in various normal tissues, GCs, and CRCs by

quantitative reverse transcriptase–polymerase chain reaction (RT-PCR) and immunohistochemistry. The aim of this study is to clarify whether claudin-2 expression is specific for cancer by comparing the expression level of claudin-2 in various normal tissues with that in cancer tissues.

Materials and methods

Tissue samples

For quantitative RT-PCR, five GCs and nine CRCs were used. The samples were obtained at the time of surgery at the Hiroshima University Hospital and affiliated hospitals. We confirmed microscopically that the tumor specimens consisted mainly (>50%) of carcinoma tissue. Samples were frozen immediately in liquid nitrogen and stored at −80°C until use. Noncancerous samples of the heart, lung, stomach, small intestine, colon, liver, pancreas, kidney, bone marrow, peripheral leukocytes, spleen, skeletal muscle, brain, and spinal cord were purchased directly from Clontech (Palo Alto, CA, USA).

For immunohistochemical analysis, we used archival formalin-fixed, paraffin-embedded tissues from 245 patients who had undergone surgical excision or removal of the tumor by polypectomy for GC (n=146) and CRC (n=99). The 146 GCs were either histologically classified (n=85) or poorly (n=61) differentiated. Ninety-nine CRCs were either histologically classified (n=47) or moderately (n=45) or poorly (n=7) differentiated. Tumor staging was carried out according to the tumor–node–metastasis (TNM) staging system [12]. Because written informed consent was not obtained, for strict privacy protection, identifying information for all samples was removed before analysis; the procedure was in accordance with the Ethical Guidelines for Human Genome/Gene Research enacted by the Japanese Government.

Cell lines

Eight cell lines derived from human GC were used. The TMK-1 cell line was established in our laboratory [16]. Five GC cell lines of the MKN series were kindly provided by Dr. T. Suzuki. KATO-III and HSC-39 cell lines were kindly provided by Dr. M. Sekiguchi and Dr. K. Yanagihara [25], respectively. All cell lines were maintained in RPMI 1640 (Nissui Pharmaceutical Co., Ltd., Tokyo, Japan) containing 10% fetal bovine serum (Whittaker, Walkersville, MA, USA) in a humidified atmosphere of 5% CO_2 and 95% air at 37°C.

Quantitative RT-PCR analysis

Total RNA was extracted with an RNeasy Mini kit (Qiagen, Valencia, CA, USA), and 1 μg of total RNA was converted to cDNA with a First-Strand cDNA Synthesis kit (Amersham Pharmacia, Little Chalfont, UK). PCR was performed with an SYBR Green PCR Core Reagents kit (Applied Biosystems, Foster City, CA, USA). Real-time detection of the emission intensity of SYBR green bound to double-stranded DNA was performed with an ABI PRISM 7700 Sequence Detection System (Applied Biosystems) as described previously [11]. *Claudin-2* cDNA and internal control cDNAs [β-actin gene (*ACTB*) and glyceraldehyde-3-phosphate dehydrogenase (*GAPDH*)] were PCR-amplified separately. Relative gene expression was determined by the threshold cycles for the *claudin-2* and *ACTB* or *GAPDH* genes. Reference samples (GC cell line, KATO-III) were included on each assay plate to verify plate-to-plate consistency. Plates were normalized to each other by these reference samples. PCR amplification was performed according to the manufacturer's instructions in 96-well optical trays with caps with a 25-μl final reaction mixture. Quantitative RT-PCRs were performed in triplicate for each sample primer set, and the mean of the three experiments was used as the relative quantification value. *Claudin-2* primer sequences are forward primer 5′-TCCCCAAACCC ACTAATCACA-3′ and reverse primer 5′-CCAACCTCAG CCAGAGAGAGG-3′. *ACTB* primer sequences were 5′-T CACCGAGCGCGGCT-3′ and 5′-TAATGTCACGCAC GATTTCCC-3′ [11]. *GAPDH* primer sequences were 5′-GGTGAAGGTCGGAGTCAACG-3′ and 5′-AGAGTTAA AAGCAGCCCTGGTG-3′. The units are arbitrary, and we calculated *claudin-2* mRNA expression by standardization to 1.0 μg total RNA from KATO-III as 1.0. We found a similar result in both quantitative RT-PCR analyses of *claudin-2* and *ACTB* or *GAPDH* of 8 GC cell lines, 14 various normal tissues, 5 GC tissues, and 9 CRC tissues. Therefore, throughout this article, we will describe and discuss the results obtained using *ACTB* as an internal control in quantitative RT-PCR analysis.

Western blot analysis

Preparation of whole cell lysates from GC cell lines was made and Western blotting was performed as described previously [26]. Protein concentrations were determined by Bradford protein assay (Bio-Rad, Hercules, CA, USA) with bovine serum albumin used as the standard. Lysates (20 μg) were solubilized in Laemmli's sample buffer by boiling and then subjected to 12% sodium dodecyl sulfate–polyacrylamide gel electrophoresis (SDS-PAGE) followed by electrotransfer onto a nitrocellulose filter. Anti-claudin-2 polyclonal antibody was purchased from Zymed (South San Francisco, CA, USA), and anti-β-actin mouse monoclonal antibody was purchased from Sigma (USA). Peroxidase-conjugated anti-rabbit IgG and anti-mouse IgG was used in the secondary reaction, respectively. The immunocomplex was visualized with an ECL Western Blot Detection System (Amersham Pharmacia Biotech).

Immunohistochemistry

A Dako LSAB kit (Dako, Carpinteria, CA, USA), which is based on the LSAB method, was used for the immunohistochemical analysis. In brief, microwave pretreatment in citrate buffer was performed for 15 min to retrieve antigenicity. After blocking the peroxidase with 3% H_2O_2–methanol for 10 min, sections were incubated with antibody/rabbit polyclonal anti-claudin-2, 1:100 (Zymed).

Sections were treated consecutively at room temperature with primary antibody for 2 h, followed by sequential 10 min incubation with biotinylated anti-rabbit IgG and peroxidase-labeled streptavidin. Staining was completed after 10 min incubation with the substrate–chromogen solution. The sections were counterstained with 0.1% hematoxylin. The results of staining with each antibody were evaluated with reference to the percentage of stained cancer cells. The results of immunohistochemistry were graded as follows: "–," 0% to 25% of tumor cells showed immunoreactivity; "+," 25–50% of tumor cells showed immunoreactivity; "++," more than 50% of tumor cells showed immunoreactivity. We regarded "++" as positive throughout this report.

Statistical methods

Associations between clinicopathologic parameters and claudin-2 expression were analyzed by Fisher's exact test. *P* values less than 0.05 were considered statistically significant.

Results

Measurement of mRNA expression of *claudin-2* in various normal tissues, GCs, and CRCs by quantitative RT-PCR

To measure the expression levels of *claudin-2* mRNA, we performed quantitative RT-PCR on 5 GCs, 5 CRCs, and 14 normal tissue samples (heart, lung, stomach, small intestine, colon, liver, pancreas, kidney, bone marrow, peripheral leukocytes, spleen, skeletal muscle, brain, and spinal cord). The results are shown in Fig. 1. In general, the expression levels in CRCs were higher than those in GCs and normal tissues. Among the 14 normal tissues mentioned, the highest level of expression was detected in the kidney. Although obvious expression of *claudin-2* was also detected in the liver, pancreas, stomach, and small intestine, it was not as high as compared with the kidney. In the lung and skeletal muscle, a faint expression of *claudin-2* was found. There was no expression in the remaining normal tissues. Expression levels of *claudin-2* were not so different between normal stomach and GCs. While no expression of *claudin-2* was found in normal colon, two of five CRCs expressed *claudin-2* at significantly higher levels (more than 5 arbitrary units).

Expression and localization of claudin-2 in cancer cell lines

To confirm the mRNA expression of *claudin-2* in cancer cells, we performed quantitative RT-PCR in eight GC cell

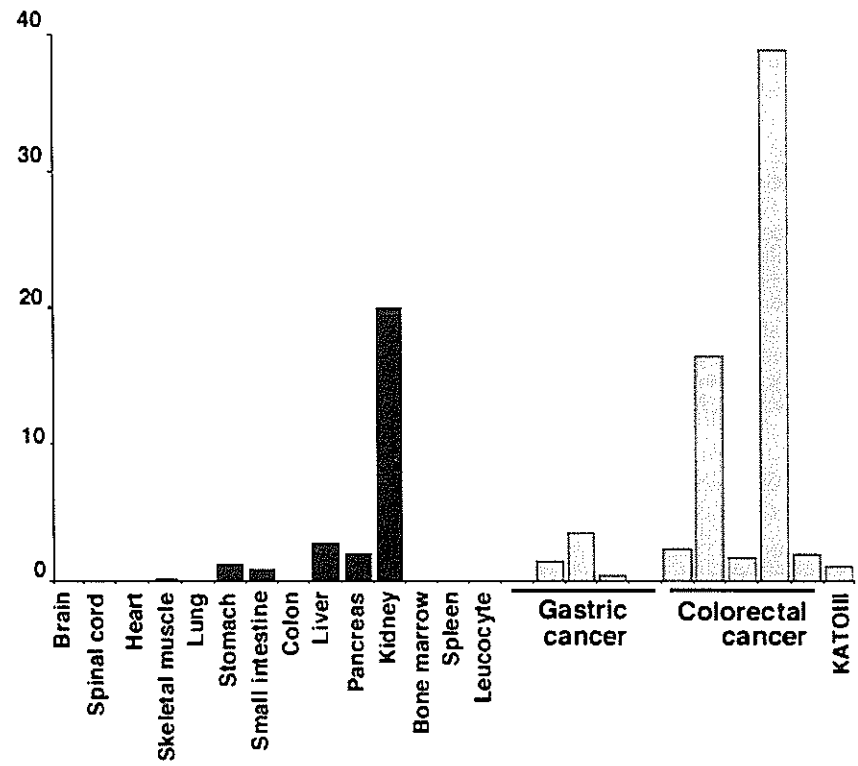

Fig. 1 Quantitative RT-PCR analysis of *claudin-2* in 14 various normal tissues as well as in 5 GC and 5 CRC samples. Among the various normal tissues, the highest level of *claudin-2* expression was found in the kidney; low expression was detected in the stomach, small intestine, liver, and pancreas; and faint expression was seen in the lung and skeletal muscle. In GCs, the expression levels were not so different from that in normal stomach. In CRCs, the expression levels were higher than those in normal colon

lines. As shown in Fig. 2a, an obvious expression of *claudin-2* was detected in MKN-45, MKN-74, and KATO-III, whereas only a low level of expression was seen in HSC-39; there was no expression detected in the remaining four GC cell lines. The anti-claudin-2 antibody detected an approximately 22-kDa band on Western blot of cell extracts from MKN-45, MKN-74, and KATO-III (Fig. 2b). We also confirmed these results by immunohistochemical staining in MKN-28 and MKN-45 cell lines. Claudin-2 staining was detected in cell membranes in MKN-45 cells but not in MKN-28 cells (Fig. 2c). Thus, this antibody was considered to be useful in the detection of claudin-2 protein in situ.

Expression and localization of claudin-2 in CRC tissues

To predict the sensitivity of anti-claudin-2 rabbit polyclonal antibody in immunohistochemistry, we examined the mRNA expression and protein expression of claudin-2 in an additional four CRC tissues. Firstly, we performed quantitative RT-PCR to detect *claudin-2* mRNA expression level and found an obvious expression of *claudin-2* (more than 5 arbitrary units) in three of four examined CRC tissue samples (Fig. 3a). The anti-claudin-2 antibody detected an approximately 22-kDa band on Western blot of protein extracts from the three CRC tissues, which showed obvious high expression in quantitative RT-PCR analysis (Fig. 3b). We also confirmed these results by immunohistochemical staining. Claudin-2 staining was detected in cell membranes of the same three CRC tissue samples, which expressed claudin-2 at a significantly higher level in both quantitative RT-PCR and Western blotting analyses (Fig. 4c). Therefore, in these CRC tissue samples, we found a good correlation between mRNA and protein levels. This result also suggests that in immunohistochemical analysis, our antibody may detect claudin-2 protein expression at levels higher than 5 arbitrary units measured by quantitative RT-PCR analysis.

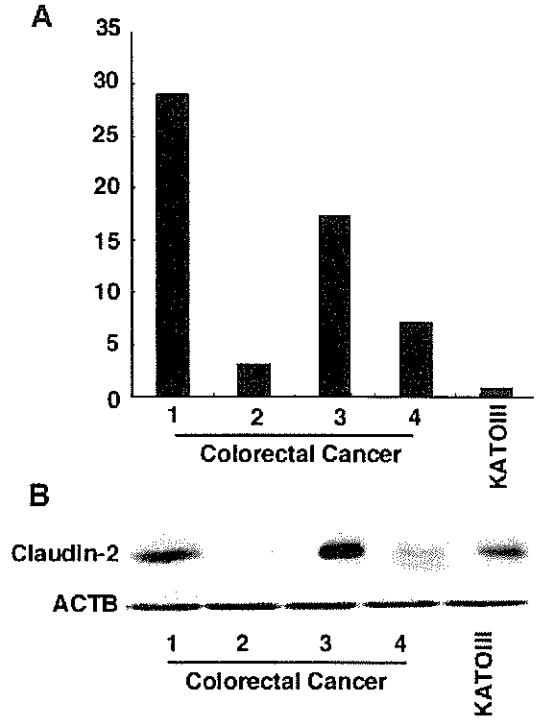

Fig. 3 Expression of claudin-2 in CRC tissue samples. Claudin-2 expression was analyzed at the mRNA level by quantitative RT-PCR (**a**) and at the protein level by Western analysis (**b**)

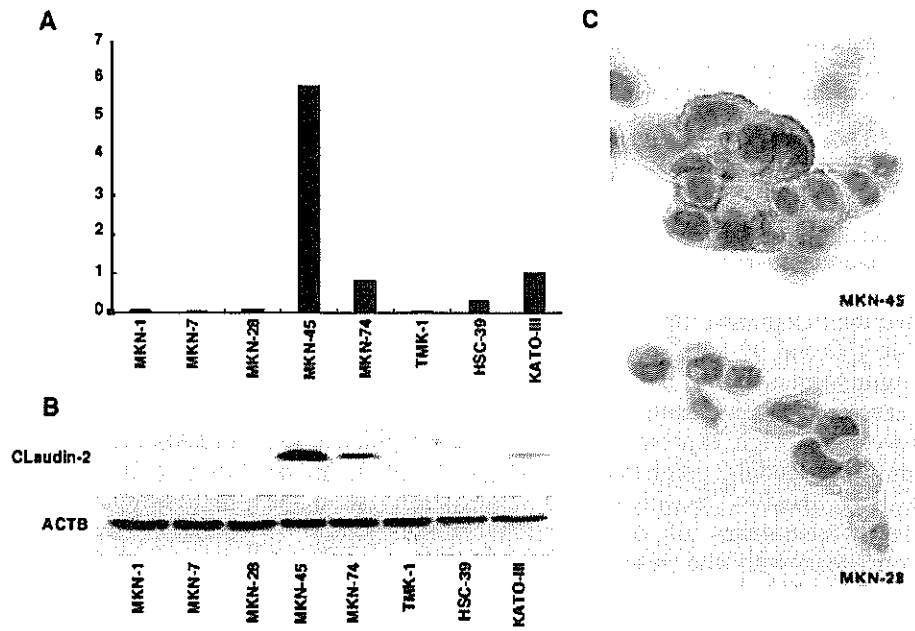

Fig. 2 Expression and localization of claudin-2 in GC cell lines. Claudin-2 expression was analyzed at the mRNA level by quantitative RT-PCR (**a**) and at the protein level by Western analysis (**b**) and immunohistochemistry (**c**); claudin-2 immunoreactivity was evident in the cell membranes of MKN-45 cells but not MKN-28 cells

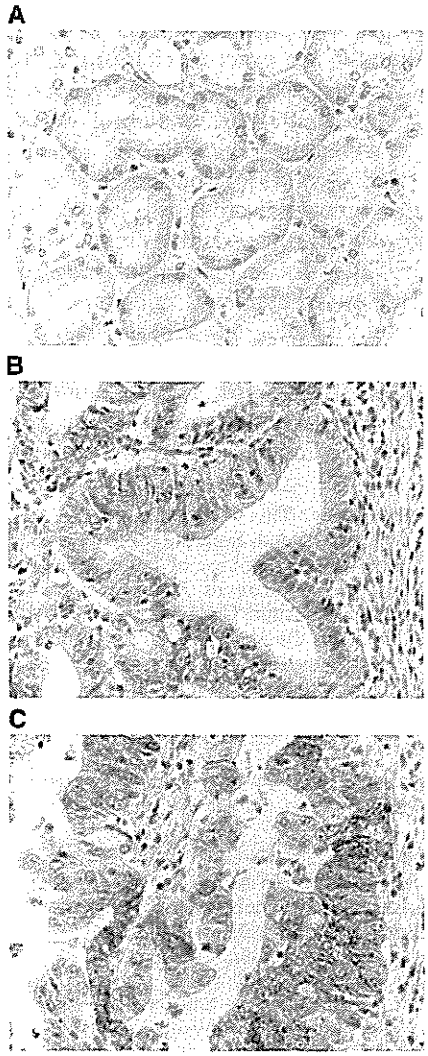

Fig. 4 Immunohistochemical analysis of claudin-2 in normal kidney (as a control) as well as in GC and CRC tissues. Staining for claudin-2 was observed in the basal membranes of the proximal tubule of the kidney (**a**), the cellular membrane of GC cells forming a tubular structure (**b**), and the cellular membrane of CRC cells forming a papillotubular structure (**c**). **c** is case number 1, which expressed *claudin-2* at a high level (more than 5 arbitrary units measured by quantitative RT-PCR), as shown in Fig. 3a,b. Original magnification was ×400

Expression of claudin-2 protein in GCs and CRCs by immunohistochemistry

We then examined the expression of claudin-2 protein in 146 GC and 99 CRC samples by immunohistochemistry. Immunostaining was also performed in normal kidney to serve as a positive control because our real-time RT-PCR revealed a high expression level and a previous report showed claudin-2 expression in mouse nephron. In the kidney, claudin-2 positivity was found strongest in the basal membranes of the proximal tubule, which is consistent with the result of previous reports [3, 9] (Fig. 3a). No obvious staining of claudin-2 was found in normal liver, stomach, and small and large intestines (data not shown). Of the 146 cases of GC, only 3 (2.1%) were positive for claudin-2. Immunoreactivity of claudin-2 was mainly observed in the cell membranes of GC cells forming a tubular structure (Fig. 3b). In CRCs, 25 (25.3%) of 99 cases were positive for claudin-2. Claudin-2 was mainly localized in the cell membranes of tumor cells forming a papillotubular structure (Fig. 3c).

We analyzed the relation between the expression of claudin-2 and clinicopathologic characteristics of CRC. There was no clear correlation between claudin-2 staining and clinicopathological parameters such as location, T grade, N grade, M grade, stage, and histologic differentiation (Table 1).

Table 1 Relation between claudin-2 protein expression and clinicopathologic characteristics in CRCs

	Claudin-2 expression	*P* value[a]
Location		
Right	8/32 (25.0%)	1.0000
Left	17/67 (25.4%)	
T grade		
T1/2	7/29 (24.1%)	1.0000
T3/4	18/70 (25.7%)	
N grade		
N0	17/58 (29.3%)	0.3494
N1/2	8/41 (19.5%)	
M grade		
M0	25/95 (26.3%)	0.5695
M1	0/4 (0.0%)	
Stage		
I	6/25 (24.0%)	0.1453
II	11/33 (33.3%)	
III	8/37 (21.6%)	
IV	0/4 (0.0%)	
Histology		
Well	14/47 (29.8%)	0.4774
Moderate	9/45 (20.0%)	
Poor	2/7 (28.6%)	

[a]Fisher's exact test

Discussion

Cellular tight junctions are structures that help preserve the integrity of cellular layers and regulate their permeability [23, 24]. It may be hypothesized that changes in expression of tight junctional proteins can lead to cellular disorientation and detachment, which are commonly seen in neoplasia. In this study, we demonstrated for the first time the expression of *claudin-2* mRNA in normal human kidney, liver, pancreas, and so on. Among these, the highest level of expression was detected in the kidney. In addition, an obvious expression of *claudin-2* was also detected in the stomach and small intestine. These results are consistent with a previous report in rat and mice; *claudin-2* is expressed in nephron, liver, pancreas, and gut

[3, 17]. We found a basal expression of claudin-2 in kidney tubules, although claudin-2 is not a known basal membrane protein and tight junctions are not known to be in the region of basal membrane. We could not explain well this unusual expression. However, it has been already published by Kiuchi-Saishin et al. [9] that claudin-2, claudin-10, and claudin-11 were clearly concentrated at the tight junction of epithelial cells of the proximal tubules. Among these, only claudin-2 seemed to be distributed along basal plasma membranes in addition to tight junction. This staining is specific for claudin-2 because the kidneys of claudin-2-deficient mice demonstrated no such staining (Furuse et al., unpublished data) [9].

We also investigated claudin-2 expression in 146 GC and 99 CRC cases to evaluate their differential expression of claudin-2 in gastrointestinal cancers. In previous studies, type-specific expression of claudin-1, claudin-2, claudin-3, claudin-4, claudin-5, and claudin-7 has been detected in various types of cancers including carcinomas of breast, pancreas, liver, esophagus, etc. [20, 21]. Soini [21] also analyzed claudin-2 expression in a small number of GCs and CRCs by using the monoclonal anticlaudin-2 antibody and reported that 12 of 13 GCs (92%) and 9 of 11 CRCs (82%) were positive for claudin-2. No method other than immunohistochemistry was utilized. In our study, the frequency of claudin-2 expression in GC and CRC was much lower as compared to the above studies, partly due to the different antibody used. However, our immunohistochemistry must be precise even if it was not so sensitive because we have found a good correlation between levels of *claudin-2* mRNA expression and protein expression by immunostaining and Western analysis of not only GC cell lines but also CRC tissues, as shown in Figs. 2, 3, and 4c. Our antibody may detect claudin-2 expression at levels higher than 5 arbitrary units, as measured by quantitative RT-PCR. In situ hybridization experiments may help detect the expression of claudin-2 with high sensitivity. We will perform it in a future study of claudin-2.

The results of the present study demonstrated that expression of claudin-2 was detected in CRCs, whereas no expression of claudin-2 was detected in normal colon. We did not find any significantly different expression between GC and normal stomach. Therefore, the participation of claudin-2 in tumorigenesis may involve organ specificity. Claudin species have been found to be the major constituents of tight junction strands [2, 5, 9, 19]. The presence of junctional claudin-2 causes the formation of cation-selective channels sufficient to transform a "tight" junction into a "leaky" one [1]. In carcinogenesis of CRC, claudin-2 may contribute to an easier leak of tight junctions in between neoplastic cells. Although we observed claudin-2 staining mainly in the neoplastic cells forming a tubular or papillary structure in both GCs and CRCs, we did not find any significant correlation between claudin-2 protein expression and histological differentiation. Moreover, we could not find any correlation with tumor advancement. Therefore, increased expression of claudin-2 may participate in the development but not in the progression of CRCs, although the exact mechanism is unknown. It has been shown that human claudin-2 promoter activity is positively regulated by the caudal-related homeobox gene (*CDX2*), as well as by the hepatocyte nuclear factor-1 alpha isoform (HNF-1α) [18]. A published study has shown the presence of functional cross talk between *CDX2* and the Wnt pathway in the positive regulation of claudin-2 expression [14]. These regulations may be the cause of the involvement of claudin-2 in colorectal carcinogenesis. In fact, abnormalities in Wnt signaling, including β-catenin/TCF, have been shown to participate in the pathogenesis of CRC [6]. Further studies are needed to explore the exact mechanism of claudin-2 involvement in gastrointestinal tumor pathology.

Acknowledgements This work was supported, in part, by Grants-in-Aid for Cancer Research from the Ministry of Education, Culture, Science, Sports, and Technology of Japan and from the Ministry of Health, Labor, and Welfare of Japan. We thank Mr. Masayoshi Takatani and Ms. Mutsumi Ueda for excellent technical assistance and advice. We thank the Analysis Center of Life Science, Hiroshima University, for the use of their facilities. The experiments in this study were in accordance with the Ethical Guidelines for Human Genome/Gene Research enacted by the Japanese government.

References

1. Amasheh S, Meiri N, Gitter AH, Schoneberg T, Mankertz J, Schulzke JD, Fromm M (2002) Claudin-2 expression induces cation-selective channels in tight junctions of epithelial cells. J Cell Sci 115:4969–4976
2. Colegio OR, Van Itallie C, Rahner C, Anderson JM (2003) Claudin extracellular domains determine paracellular charge selectivity and resistance but not tight junction fibril architecture. Am J Physiol Cell Physiol 284:C1346–C1354
3. Enck AH, Berger UV, Yu AS (2001) Claudin-2 is selectively expressed in proximal nephron in mouse kidney. Am J Physiol Renal Physiol 281:F966–F974
4. Furuse M, Sasaki H, Fujimoto K, Tsukita S (1998) A single gene product, claudin-1 or -2, reconstitutes tight junction strands and recruits occludin in fibroblasts. J Cell Biol 143:391–401
5. Furuse M, Sasaki H, Tsukita S (1999) Manner of interaction of heterogeneous claudin species within and between tight junction strands. J Cell Biol 147:891–903
6. Gaspar C, Fodde R (2004) APC dosage effects in tumorigenesis and stem cell differentiation. Int J Dev Biol 48(5–6):377–386
7. Hough CD, Sherman-Baust CA, Pizer ES, Montz FJ, Im DD, Rosenshein NB, Cho KR, Riggins GJ, Morin PJ (2000) Large-scale serial analysis of gene expression reveals genes differentially expressed in ovarian cancer. Cancer Res 60(22):6281–6287
8. Itoh M, Furuse M, Morita K, Kubota K, Saitou M, Tsukita S (1999) Direct binding of three tight junction-associated MAGUKs, ZO-1, ZO-2, and ZO-3, with the COOH termini of claudins. J Cell Biol 147:1351–1363
9. Kiuchi-Saishin Y, Gotoh S, Furuse M, Takasuga A, Tano Y, Tsukita S (2002) Differential expression patterns of claudins, tight junction membrane proteins, in mouse nephron segments. J Am Soc Nephrol 13:875–886
10. Kominsky SL, Argani P, Korz D, Evron E, Raman V, Garrett E, Rein A, Sauter G, Kallioniemi OP, Sukumar S (2003) Loss of the tight junction protein claudin-7 correlates with histological grade in both ductal carcinoma in situ and invasive ductal carcinoma of the breast. Oncogene 22(13):2021–2033

11. Kondo T, Oue N, Yoshida K, Mitani Y, Naka K, Nakayama H, Yasui W (2004) Expression of POT1 is associated with tumor stage and telomere length in gastric carcinoma. Cancer Res 64:523–529
12. Lauren P (1965) The two histological main types of gastric carcinoma: diffuse and so-called intestinal-type carcinoma an attempt at a histo-clinical classification. Acta Pathol Microbiol Scand 64:31–49
13. Long H, Crean CD, Lee WH, Cummings OW, Gabig TG (2001) Expression of Clostridium perfringens enterotoxin receptors claudin-3 and claudin-4 in prostate cancer epithelium. Cancer Res 61(21):7878–7881
14. Mankertz J, Hillenbrand B, Tavalali S, Huber O, Fromm M, Schulzke JD (2004) Functional crosstalk between Wnt signaling and Cdx-related transcriptional activation in the regulation of the claudin-2 promoter activity. Biochem Biophys Res Commun 314:1001–1007
15. Michl P, Barth C, Buchholz M, Lerch MM, Rolke M, Holzmann KH, Menke A, Fensterer H, Giehl K, Lohr M, Leder G, Iwamura T, Adler G, Gress TM (2003) Claudin-4 expression decreases invasiveness and metastatic potential of pancreatic cancer. Cancer Res 63(19):6265–6271
16. Ochiai A, Yasui W, Tahara E (1985) Growth-promoting effect of gastrin on human gastric carcinoma cell line TMK-1. Jpn J Cancer Res 76:1064–1071
17. Rahner C, Mitic LL, Anderson JM (2001) Heterogeneity in expression and subcellular localization of claudins 2, 3, 4, and 5 in the rat liver, pancreas, and gut. Gastroenterology 120:411–422
18. Sakaguchi T, Gu X, Golden HM, Suh E, Rhoads DB, Reinecker HC (2002) Cloning of the human claudin-2 5′-flanking region revealed a TATA-less promoter with conserved binding sites in mouse and human for caudal-related homeodomain proteins and hepatocyte nuclear factor-1alpha. J Biol Chem 277:21361–21370
19. Sasaki H, Matsui C, Furuse K, Mimori-Kiyosue Y, Furuse M, Tsukita S (2003) Dynamic behavior of paired claudin strands within apposing plasma membranes. Proc Natl Acad Sci U S A 100:3971–3976
20. Soini Y (2004) Claudins 2, 3, 4, and 5 in Paget's disease and breast carcinoma. Hum Pathol 35:1531–1536
21. Soini Y (2005) Expression of claudins 1, 2, 3, 4, 5 and 7 in various types of tumors. Histopathology 46:551–560
22. Terris B, Blaveri E, Crnogorac-Jurcevic T, Jones M, Missiaglia E, Ruszniewski P, Sauvanet A, Lemoine NR (2002) Characterization of gene expression profiles in intraductal papillary-mucinous tumors of the pancreas. Am J Pathol 160(5):1745–1754
23. Tsukita S, Furuse M (2000) Pores in the wall: claudins constitute tight junction strands containing aqueous pores. J Cell Biol 149:13–16
24. Tsukita S, Furuse M (2002) Claudin-based barrier in simple and stratified cellular sheets Curr Opin Cell Biol 14(5):531–536
25. Yanagihara K, Seyama T, Tsumuraya M, Kamada N, Yokoro K (1991) Establishment and characterization of human signet ring cell gastric carcinoma cell lines with amplification of the c-myc oncogene. Cancer Res 51:381–386
26. Yasui W, Ayhan A, Kitadai Y, Nishimura K, Yokozaki H, Ito H, Tahara E (1993) Increased expression of p34cdc2 and its kinase activity in human gastric and colonic carcinomas. Int J Cancer 53:36–41

Demethylation of promoter C region of estrogen receptor α gene is correlated with its enhanced expression in estrogen-ablation resistant MCF-7 cells

Tetsuya Sogon[a,b], Shigeru Masamura[c], Shin-ichi Hayashi[d], Richard J. Santen[e], Kei Nakachi[a,b], Hidetaka Eguchi[a,b,*]

[a] *Department of Molecular Epidemiology, Hiroshima University Graduate School of Biomedical Sciences and*
[b] *Department of Radiobiology/Molecular Epidemiology, Radiation Effects Research Foundation, 5-2, Hijiyama-park, Minami-ku, Hiroshima, 732-0815, Japan*
[c] *Department of Surgery, Tokyo Dental College Ichikawa General Hospital, 5-11-13, Sugano, Ichikawa, Chiba, 272-8513, Japan*
[d] *Department of Medical Technology, Tohoku University School of Medicine, 2-1, Seiryocho, Aoba-ku, Sendai, 980-8575, Japan*
[e] *University of Virginia Health System, Charlottesville, Virginia 22908, USA*

Abstract

Long-term estrogen deprivation (LTED) MCF-7 cells showing estrogen-independent growth, express estrogen receptor (ER) α at a much higher level than wild-type MCF-7 cells. Enhanced expression of ERα associated with partial localization of ERα to the plasma membranes in LTED cells is thought to be an important step for acquisition of estrogen-ablation resistance.

In this study, we compared the regulation of ERα gene expression between wild-type and LTED cells, examining the usage of the promoters A and C as well as their methylation status. We found that transcription from the promoter C was drastically enhanced in LTED cells, compared with that in wild-type cells. Furthermore, the promoter C region was highly unmethylated in LTED cells, but partially methylated in wild-type cells.

Our findings imply that demethylation of promoter C region in the ERα gene is in part responsible for the enhanced expression of ERα gene in LTED cells.

J Steroid Biochem Mol Biol, in press.

Keywords: estrogen receptor α; breast cancer; methylation

1. Introduction

Experimental, clinical, and epidemiologic data suggest that estrogens contribute to the development of breast cancer. Estrogens bind to ER α or β and stimulate the transcription of target genes involved in cell proliferation. Thus the anti-estrogen therapy such as tamoxifen has been generally used for ERα-positive breast cancer for several decades. Recently, clinical trials in the adjuvant, neoadjuvant and advanced disease setting have demonstrated a greater clinical efficacy of the aromatase inhibitors aiming to decrease the concentration of estrogen, compared with selective estrogen receptor modulators represented by tamoxifen [1,2].

*Corresponding author: Hidetaka Eguchi, Department of Molecular Epidemiology, Hiroshima University Graduate School of Biomedical Sciences and Department of Radiobiology/Molecular Epidemiology, Radiation Effects Research Foundation, 5-2, Hijiyama-park, Minami-ku, Hiroshima 732-0815, Japan. Tel.: +81-82-261-3169; fax: +81-82-261-3170. *E-mail address*: eguchi@rerf.or.jp (H. Eguchi).

On the other hand, clinical observations suggested that some human breast cancers adapted to hormone-ablative therapy involving surgically deprivation of estrogen production. Hormone-dependent breast cancers often regress in response to surgical removal of the ovaries, a treatment which lower circulating plasma estradiol (E2) from approximately 200 to 15 pg/ml [3]. In response to this acute deprivation of E2, tumors regress for 12-18 months on average before they begin to regrow. Second-line therapy with surgical oophorectomy or with aromatase inhibitors can then induce additional tumor regression by lowering E2 concentrations further to 1-5 pg/ml [4]. These observations for the first time demonstrated enhanced sensitivity to circulating E2.

In order to demonstrate the phenomenon of adaptive hypersensitivity and to determine the mechanisms involved, we have established a model system involving MCF-7 human breast cancer cells *in vitro*. Wild-type MCF-7 cells were cultured over a prolonged period in estrogen-free medium to mimic the effect of ablative endocrine therapy such as induced by surgical oophorectomy [5]. This process involves long-term E2 deprivation; the adapted cells are called by LTED cells. When LTED cells were cultured in the presence of E2 for 4 months, the cells showed estrogen-dependent growth as was observed for wild-type MCF-7 cells [5].

Importantly, ERα is expressed at a much higher level in LTED cells than in wild-type MCF-7 cells [6]. In concert with this observation, an elevated basal ER transactivation activity (mean increase; 5 fold) was measured in LTED cells compared with the wild-type cells using pERE-tk-CAT, a reporter gene driven by estrogen responsive element-thymidine kinase promoter [6] .

In addition to the established role as a nuclear receptor, ERα may have another function on the plasma membrane. In LTED cells, ERα localizes predominantly to the nuclei and some also present on the plasma membranes [7]. The subcellular localization of ERα to the plasma membranes in LTED cells may, at least in part, be due to the enhanced expression of ERα in LTED cells, since plasma membrane-associated ERα can only be observed in ERα-enriched MCF-7 sub-cell lines (mER^{high}) but not ERα-depleted ones ($mER\alpha^{low}$) [8]. Constitutively activated MAP kinase activity was observed in LTED cells independent of serum factors [9]. A rapid physical interaction of the plasma membrane-associated ERα and an adaptor protein Shc has been observed upon addition of E2 [7]; Shc is subsequently phosphorylated and triggers the MAP kinase signaling pathway [10,11].

Thus, when ERα works as a transcription factor in the nuclei and also as a signal transducer on the plasma membranes, typically in LTED cells, enhanced expression of ERα may be an obligatory step for acquisition of estrogen-ablation resistance. Though, the mechanisms how ERα expresses at high level in LTED cells still remain unknown.

Several human ERα gene promoters (A to F) are identified so far [12]. These promoters are differently utilized in a tissue- and cell-dependent manner [13,14,15]. Among these promoters, we previously demonstrated that the transcript from promoter A was constitutively used in both normal and cancerous mammary tissue, while the transcript from promoter C (formerly called promoter B) showed remarkable correlation to the ERα protein levels in ERα-positive breast cancer [16]. Furthermore, we have identified a *cis*-acting element, ERBF-1, that plays an important role in the expression of the ERα gene transcribed from promoter C in breast cancer cells [17]. On the other hand, a transcription factor ERF-1, a member of AP2 transcription factor, is important for the transcriptional regulation of promoter A [18,19]. In addition, methylation of the promoter A and C regions was critical for the repression of gene transcription from these promoters [20]. Collectively, methylation of these promoter regions as well as alteration of critical transcription factors are thought to be important for ERα gene expression in breast cancer cells.

In this study, we examined regulation of ERα gene expression in wild-type MCF-7 and LTED cells. We first found that transcription from the promoter C was drastically enhanced in LTED cells, compared with that in the wild-type cells. Transient transfection with a reporter gene driven by the promoter A or promoter C of ERα gene revealed that transcription factors are equally available in these cells. Second, differences in epigenetic alterations of promoter C were found between LTED and wild-type cells: The promoter C region was highly unmethylated in LTED cells, while that in wild-type cells was partially methylated. Our findings imply that demethylation of promoter C region in the ERα gene is in part responsible for the enhanced expression of ERα gene in LTED cells.

2. Materials and methods

2.1. Tissue culture

Human breast cancer cells wild-type MCF-7 were maintained in improved MEM (IMEM) containing 5% dextran-coated charcoal-stripped fetal bovine serum (DCC-FBS) and 10 nM E2. LTED cells were established by long-term culture of wild-type MCF-7 cells in IMEM containing 5% DCC-FBS. The established LTED cells were stored in liquid nitrogen until use. LTED cells were maintained in IMEM containing 5% DCC-FBS.

2.2. Plasmid

Reporter plasmids pGL3-ProA 1.3K and pGL3-ProC (formerly called pGL3-ProB1.4K) were described previously [20]. An internal control pRL-TK was purchased from Promega (Madison, WI).

2.3. *RNA extraction and cDNA synthesis*

Total RNA was prepared from wild-type and LTED cells using RNeasy Mini kit (QIAGEN, Hilden, Germany). One μg of total RNA was reverse transcribed with Quantitect Reverse Transcription (QIAGEN) using RT primer mix as primers in a final volume of 20 μl at 42°C for 15 min.

2.4. Real-time PCR analysis of ERα mRNA expression

The real-time PCR was performed in tripicate using iCycler iQ (Bio-Rad Laboratories, Hercules, CA). Reaction mixture consisted of 1 μl of cDNA products, 0.5 μl of each primers and 12.5 μl of SYBR Green ROX Mix (ABgene, Epsom, UK) in a total volume of 25 μl. PCR thermal conditions were as following: 95°C for 15 min for 1 cycle and 95°C for 20 sec, 60°C for 15 sec, 72°C for 10 sec, and 86°C for 15sec (fluorescent signal collection) for 50 cycles for detection of ERα mRNA from promoters A and C; 95°C for 15 min for 1 cycle and 94°C for 15 sec, 68°C for 30 sec, and 86°C for 15 sec (fluorescent signal collection) for 50 cycles for detection of total ERα mRNA. The following primers were used: PROA1, 5'-ACC TCG GGC TGT GCT CTT-3' and PRODW, 5'-GAG GGT CAT GGT CAT GGT-3' for ERα mRNA from promoter A; PROB3, 5'-GCC CAG GAA CAT TTC TGG AA-3' and PRODW for ERα mRNA from promoter C; EREX1, 5'-AGA ACG AGC CCA GCG GCT AC-3' and EREX2-R, 5'-CCT TGC AGC CCT CAC AGG AC-3' for total ERα mRNA. For construction of standard curves, serially diluted plasmids harboring fragment of target gene sequences were used after digestion with *Not* I restriction enzyme to release the insert fragments. As a control, β-actin mRNA was also measured as described previously [21].

2.5. Transient transfection assays

A transient transfection of the plasmids was performed in triplicate using SuperFect Transfection Reagent (QIAGEN) under manufacturer's instruction. Briefly, $1x10^5$ cells were plated onto 24 wells plastic dish. After over night culture, 1 μg of pGL3-ProA1.3K or pGL3-ProC and 0.1 μg of pRL-TK were mixed with 5 μl of the SuperFect Transfection Reagent in 350 μl of the medium with 5% DCC-FBS and subjected to transfection. After two hours incubation, the medium was replaced with a fresh medium and cells were incubated for 48 hours. Then, cells were collected and lysed using Passive Lysis Buffer (Promega). Luciferase assays were performed using Dual-Luciferase Reporter Assay System (Promega) and TD-20/20 Luminometer (TURNER DESIGNS, CA).

2.6. Bisulfite modification and methylation-specific PCR

Total DNA was extracted from wild-type and LTED cells using NucleoSpin Tissue (MACHEREY-NAGEL, Düren, Germany). DNA was subjected to bisulfite conversion using EZ DNA Methylation kit (ZYMO Research, Orange, CA) according to the manufacture's instruction, essentially based on the report by Herman *et al.* [22]. Briefly, after denaturation with NaOH, 500 ng of DNA was incubated in a buffer containing sodium bisulfite at 50°C for 16 hours, followed by purification using ZYMO-Spin I column. Bisulfite-converted DNA was eluted in 10 μl of M-Elution buffer. First PCR amplification aiming to amplify bisulfite-converted DNA fragments was performed in 20 μl of reaction mixture containing 1 μl of bisulfite-treated genomic DNA, 0.5 μM each primers, 0.2 mM dNTPs, 2.5 mM $MgCl_2$ and 1.25 units of AmpliTaq Gold DNA polymerase (Applied Biosystem, Foster, CA) under the following conditions: 95°C for 5 min for 1 cycle and 95°C for 15 sec, 54°C for 15 sec, and 72°C for 1 min for 35 cycles. Second PCR amplification using methylation- or unmethylation-specific primers was performed in 20 μl of reaction mixture containing 1 μl of first PCR product (1/100 diluted with MilliQ water), 0.5 μM each primers, 0.2 mM dNTPs, 2.5 mM $MgCl_2$ and 1.25 units of AmpliTaq Gold DNA polymerase under the following conditions: 95°C for 5 min for 1 cycle and 95°C for 15 sec, 57°C (methylation) or 54°C (unmethylation) for 30 sec, and 72°C for 20 sec for 35 cycles. The amplified fragments were electrophoresed to 8% polyacrylamide gel. All the primers used for this methylation analysis were designed using MethPrimer [23]. Primers used for the first PCR and second PCR are summarized in Table 1.

For quantification, real-time PCR amplification was performed in 25 μl of reaction mixture containing 1 μl of the first PCR product (1/100 diluted with MilliQ water), 0.2 μM each primers and 12.5 μl of SYBR Green Rox Mix according to the manufacturer's protocol using iCycler iQ under the following conditions: 95°C for 15 min for 1 cycle and 95°C for 15 sec, 57°C (methyl) or 54°C (unmethyl) for 15 sec, 72°C for 15 sec, and fluorescent signal collection at 77°C (methyl) or 76°C (unmethyl) for 20 sec for 40 cycles. The assay was conducted in triplicate and repeated for three times. For construction of a standard curve, serially diluted control PCR fragments were used.

2.7. Bisulfite-sequencing and combined bisulfite restriction analysis (COBRA)

PCR amplification of ERα promoter C region using bisulfite-converted DNA fragments was performed as described above except for the cycle numbers to be 50. The amplified fragments were purified using NucleoSpin Extract II kit (MACHEREY-NAGEL). Direct sequencing of the fragments was conducted using ERPROCBSF as a primer, BigDye Terminators v1.1 Cycle Sequencing Kit and ABI PRISM 310 Genetic Analyzer (Applied Biosystems, Foster City, CA). For COBRA, 5 μl of purified DNA fragment was digested in a total volume of 20 μl using 5 units of *Hpy*188III restriction enzyme (New England BioLabs, Beverlr, MA) that cleave CpG sites retained because of methylation at 37°C for 4 hours. The resultant DNA fragments together with undigested ones were electrophoresed onto 8% polyacrylamide gel. After staining with ethidium bromide, the image was visualized under UV illumination. Intensity of the fluorescence of each band was quantified using ChemImager 5500 (Alpha Innotech, San Leandro, CA).

2.8. Statistical analysis

Student's *t*-test was conducted for statistical analysis. When necessary, the *t*-test was modified to all for unequal variances. *P*-values less than 0.05 were considered as significant.

Table 1. Primers used for the methylation-specific PCR

Promoter	PCR	Specification	Primer name	Primer sequence	Annealing Temp. (°C)
A	1st	Bisulfite conversion specific	ERPROABSF	5'-TTAATGTTAGGGTAAGGTAATAGTTTT-3'	54
			ERPROABSR	5'-AACCACCTAAAAAAAAAACACAA-3'	
	2nd	Methylation specific	ERPROAM1F	5'-AGTTTAGGAGTTGGCGGAGGGC-3'	60
			ERPROAM1R	5'-CCGAAATTAAAAACGACGCAACG-3'	
		Unmethylation specific	ERPROAU1F	5'-GGGAGTTTAGGAGTTGGTGGAGGGT-3'	60
			ERPROAU1R	5'-ACCCAAAATTAAAAACAACACAACACA-3'	
C	1st	Bisulfite conversion specific	ERPROCBSF	5'-AGTAGATAGTAAGTTTTTTTTTATTTTTT-3'	54
			ERPROCBSR	5'-AAAAACAACCAATAAACAAAA-3'	
	2nd	Methylation specific	ERPROCM1F	5'-TTTTTTATTGTTATTTATTTAGCGT-3'	57
			ERPROCM1R	5'-AAAACACTTAACAACCCCTCCCGAC-3'	
		Unmethylation specific	ERPROCU1F	5'-TATTTTTTATTGTTATTTATTTAGTGT-3'	54
			ERPROCU1R	5'-AAACACTTAACAACCCCTCCCAAC-3'	

3. Results

3.1. Expression levels of ERα mRNA in wild-type and LTED cells

We previously demonstrated that ERα protein and mRNA were expressed at higher levels in LTED cells than in wild-type cells using Western and Northern blot analyses [6] (Jeng *et al.* 1998). As a first step, we conducted real-time PCR analysis to quantitatively evaluate ERα mRNA expression in wild-type and LTED cells: LTED cells showed 27-fold total ERα mRNA expression levels as compared with wild-type cells did (P=0.004) (Fig. 1).

Since an increase of ERα mRNA from promoter C was responsible for the enhanced expression of ERα protein in ERα-positive primary breast cancer and since promoter A was constitutively utilized in both normal and cancerous mammary tissue [16], we next compared ERα mRNA expression levels transcribed from these promoters A and C between wild-type and LTED cells using real-time PCR (Fig. 2). ERα mRNA from promoter A in LTED cells was 35-fold higher than that in wild-type cells (P = 0.0007) (Fig. 2). Furthermore, ERα mRNA expression level from promoter C in LTED was 149-fold higher than that in wild-type cells (P = 0.01) (Fig. 2). In wild-type cells, promoter A was dominant while promoters A and C were equally utilized in LTED cells (Fig. 2). These results indicate that reinforced utilization of promoter C in LTED cells as compared with wild-type cells may be important for the enhanced expression of ERα in LTED cells.

3.2. Transient transfection of reporter gene constructs with ERα gene promoters

The *cis*- and *trans*-acting factors are thought to generate differences in transcription activity on various promoters. We first tested the possibility that alterations of transcription factors may generate an increased level of ERα expression in LTED cells, compared with wild-type cells. We then measured the promoter activities in wild-type and LTED cells using reporter gene constructs driven by ERα promoters A and C. No significant differences in promoter activities between wild-type and LTED cells were observed for these two promoters (P = 0.3 and 0.1 for promoters A and C, respectively, Fig. 3), suggesting that *trans*-acting factors specific to promoters A and C are not responsible for the different utilization of ERα promoters A and C between wild-type and LTED cells.

3.3. Different methylation status of ERα gene promoters in wild-type and LTED cells

We next hypothesized that alternations of higher order chromatin structure caused by DNA methylation may contribute to the expression level of ERα in these cells. Then, we compared methylation status of ERα gene promoters A and C in wild-type and LTED cells by methylation-specific PCR. Promoter A of ERα gene was unmethylated in both wild-type and LTED cells (Fig. 4). On the other hand, promoter C of ERα gene showed partial methylation in wild-type cells (Fig. 4), in good agreement with our previous report [20]. In LTED cells, the unmethylated band for promoter C was clearly observed, while the methylated one was considerably weaker (Fig. 4), in accordance with our observation that promoter C was actively utilized in LTED cells.

In order to confirm the difference of methylation status of the promoter C between wild-type and LTED cells, we next conducted direct sequencing of the PCR fragment amplified from bisulfite-converted DNA. Cytosines were predominantly observed at nucleotides –2103, -2082, and –2073 within CpG dinucleotides, while thymines are faintly detected at these sites in wild-type cells (Fig.5). On the other hand, both thymines and cytosines were clearly observed at these sites in LTED cells (Fig.5), confirming the difference of methylation status between wild-type and LTED cells.

3.4. Quantitative analysis of methylation status of ERα gene promoter C in wild-type and LTED cells

In order to quantitatively analyze the methylation of the promoter C region, we next performed two different analyses, i.e., COBRA assay and bisulfite-real-time PCR. In COBRA assay, the fragment amplified from methylated DNA can be identified as digestible bands with restriction enzyme *Hpy*188III, because of the retention of methyl-cytosine residue at –2073 even after bisulfite-treatment (Fig.6). Quantification of the fragments revealed that 54% of the fragments were methylated in wild-type cells, while only 7.7% were methylated in LTED cells (Fig.6).

This was also examined with bisulfite-real-time PCR analysis using methylation- or unmethylation-specific primers as described above. Amount of methylated DNA in the tested sample from LTED cells was 42% of that from wild-type cells, though this was not statistically significant (P = 0.063) (Fig.7). On the other hand, unmethylated DNA amount was 14.2 fold in LTED cells as compared with wild-type cells (P < 0.001) (Fig.7). These results demonstrated that the promoter C region was highly unmethylated in LTED cells, but partially methylated in wild-type cells.

4. Discussion

Clinical observations suggest that human breast tumors can adapt to endocrine therapy by developing hypersensitivity to estrogen. To understand the mechanisms underlying this, we have previously examined estrogenic stimulation of cell proliferation in a model system and provided *in vitro* and *in vivo* evidence that long-term E2 ablation causes adaptive hypersensitivity. Importantly, LTED cells express ERα at a much higher level than wild cells and consequently show subcellular localization of ERα to the plasma membrane in addition to the nucleus. LTED cells showed higher basal estrogen responsive transcription activity as compared with wild-type cells. In addition, LTED cells activate MAP kinase signaling pathway mediated by plasma membrane-bound ERα. In both roles of ERα in the nuclei and on the plasma membranes of LTED cells, enhanced expression of ERα protein may be an obligatory step for acquisition of estrogen-ablation resistance.

Our transient transfection experiments indicated that alterations of transcription factors may not be a major cause for the enhanced expression of ERα mRNA from promoter C in LTED cells (Fig. 3). On the other hand, methylation status of the promoter C region of ERα gene was drastically changed in LTED cells as compared with wild-type cells (Figs. 4, 5, 6, 7). We have previously reported that specific *in vitro* methylation of promoter C region of ERα gene significantly reduced its promoter activity in transient transfection experiment [20]. In addition, methylation of promoter C was inversely associated with expression of transcripts from this promoter as well as ERα protein in primary breast cancer [20]. Taken together, hypomethylation of promoter C region in LTED cells can be one of the mechanisms responsible for the enhanced transcription of ERα gene from promoter C.

In this study, we demonstrated that ERα transcript from promoter A also expressed at high levels in LTED cells as compared with wild-type cells (Fig. 2). Since the promoter A was highly unmethylated in both LTED and wild-type MCF-7 cells (Fig. 4), some mechanisms other than DNA methylation should be involved in the regulation of promoter A in LTED cells. Our transient transfection experiments did not show any difference of the reporter gene activity of promoter A constructs in between LTED and wild-type MCF-7 cells (Fig. 3). One possible explanation for the enhanced expression of the transcript from promoter A in LTED cells could be alteration of transcription factors that bind to downstream sequences including intron of the ERα gene that are not present in our tested construct; AP2 transcription factor that bind to the ERF-1 *cis*-acting element located downstream of the transcription start site of promoter A may be one of the candidates [26, 27].

Transcripts from promoter A and C share an identical coding sequence for ERα protein. Then, is there any functional difference between these transcripts in relation to the protein level of ERα ? Importantly, it has recently been shown that 5' upstream open reading frame (ORF) that is specific to the transcript A has inhibitory effects on the translation of ERα protein, while the 5' upstream ORF of transcript C did not show the effect [28]. Notably, the inhibitory effect of the ORF of transcript A was most remarkable in MCF-7 cells among the tested cell lines, indicating that there are differences in the translational potential of transcripts from these two major promoters [28]. It would be interesting to test whether such regulatory effects of upstream ORF specific to transcript A is also present in MCF-7 LTED cells.

In conclusion, we found that transcription from promoters A and C were highly activated in LTED cells. Specifically, hypomethylation of promoter C correlated well with its drastically enhanced expression in LTED cells, suggesting that epigenetic alterations may play some roles in enhanced expression of ERα important for the acquisition of estrogen-ablation resistance of breast cancer cells.

Acknowledgement

We thank Ms. Shoko Hirano for her excellent technical assistance. This work was supported in part by a Grant-in-Aid for Science, Ministry of Education, Culture, Sports, Science, and Technology, Japan.

References

[1] V.C. Jordan, Selective estrogen receptor modulation: concept and consequences in cancer, Cancer Cell 5 (3) (2004) 207-213.

[2] W. Yue, J.P. Wang, Y. Li, W.P. Bocchinfuso, K.S. Korach, P.D. Devanesan, E. Rogan, E. Cavalieri, R.J. Santen, Tamoxifen versus aromatase inhibitors for breast cancer prevention, Clinical Cancer Res. 11 (2) (2005) 925-930.

[3] R.J. Santen, H.A. Harvey, Use of aromatase inhibitors in breast carcinoma, Endocr. Relat. Cancer 6 (1) (1999) 75-92.

[4] R.J. Santen, A. Manni, H.A. Harvey, C. Redmond, Endocrine treatment of breast cancer in woman, Endocr. Rev. 11 (2) (1990) 221-265.

[5] S. Masamura, S.J. Santner, D.F. Heitjan, R.J. Santen, Estrogen deprivation causes estradiol hypersensitivity in human breast cancer cells, J. Clin. Endocrinol. Metab. 80 (10) (1995) 2918-2925.

[6] M.H. Jeng, M.A. Shupnik, T.P. Bender, E.H. Westin, D. Bandyopadhyay, R. Kumar, S. Masamura, R.J. Santen, Estrogen receptor expression and function in long-term estrogen-deprived human breast cancer cells, Endocrinology 139 (10) (1998) 4164-4174.

[7] R.X. Song, R.A. McPherson, L. Adam, Y. Bao, M. Shupnik, R. Kumar, R.J. Santen, Linkage of rapid estrogen action to MAPK activation by ERα-Shc association and Shc pathway activation, Mol. Endocrinol. 16 (1) (2002) 116-127.

[8] D. Zivadinovic, C.S. Watson, Membrane estrogen receptor-α levels predict estrogen-induced ERK1/2 activation in MCF-7 cells, Breast Cancer Res. 7 (1) (2005) 130-144.

[9] W. Yue, J.P. Wang, M. Conaway, S. Masamura, Y. Li, R.J. Santen, Activation of the MAPK pathway enhances sensitivity of MCF-7 breast cancer cells to the mitogenic effort of estradiol, 143 (9) (2002) Endocrinology 3221-3229.

[10] Z. Zhang, R. Kumar, R.J. Santen, R.X. Song, The role of adapter protein Shc in estrogen non-genomic action, Steroids 69 (8-9) (2004) 523-529.

[11] R.J. Santen, R.X. Song, Z. Zhang, R. Kumar, M.H. Jeng, S. Masamura, J. Lawrence, L. Berstein, W. Yue, Long-term estradiol deprivation in breast cancer cells up-regulates growth factor signaling and enhances estrogen sensitivity, Endocr. Relat. Cancer 12 (Suppl 1) (2005) 61-73.

[12] M. Koš, G. Reid, S. Denger, F. Gannon, Minireview: genomic organization of the human ERα gene promoter region, Mol. Endocrinol. 15 (12) (2001) 2057-2063.

[13] G. Flouriot, C. Griffin, M. Kenealy, V. Sonntag-Buck, F. Gannon, Differentially expressed messenger RNA isoforms of the human estrogen receptor-α gene are generated by alternative splicing and promoter usage, Mol. Endocrinol. 12 (12) (1998) 1939-1954.

[14] A. Malyala, M.J. Kelly, O.K. Rønnekleiv, Estrogen modulation of hypothalamic neurons: activation of multiple signaling pathways and gene expression changes, Steroids 70 (5-7) (2005) 397-406.

[15] K.M. Österlund, K. Grandied, E. Keller, Y.L. Hurd, The human brain has distinct regional expression patterns of estrogen receptor α mRNA isoforms derived from alternative promoters, J. Neurochem. 75 (4) (2000) 1390-1397.

[16] S. Hayashi, K. Imai, K. Suga, T. Kurihara, Y. Higashi, K. Nakachi, Two promoters in expression of estrogen receptor messenger RNA in human breast cancer, Carcinogenesis 18 (3) (1997) 459-464.

[17] K. Tanimoto, H. Eguchi, T. Yoshida, K. Hajiro-Nakanishi, S. Hayashi,

Regulation of estrogen receptor α gene mediated by promoter B responsible for its enhanced expression in human breast cancer, Nucleic Acids Res. 27 (3) (1999) 903-909.

[18] E.C. deConinck, L.A. McPherson, R.J. Weigel, Transcriptional regulation of estrogen receptor in breast carcinomas, Mol. Cell. Biol. 15 (4) (1995) 2191-2196.

[19] L.A. McPherson, V.R. Baichwal, R.J. Weigel, Identification of ERF-1 as a member of the AP2 transcription factor family, Proc. Natl. Acad. Sci. U.S.A. 94 (9) (1997) 4342-4347.

[20] T. Yoshida, H. Eguchi, K. Nakachi, K. Tanimoto, Y. Higashi, K. Suemasu, Y. Iino, Y. Morishita, S. Hayashi, Distinct mechanisms of loss of estrogen receptor α gene expression in human breast cancer: methylation of the gene and alteration of *trans*-acting factor, Carcinogenesis 21 (12) (2000) 2193-2201.

[21] N. Yoshida, Y. Omoto, A. Inoue, H. Eguchi, Y. Kobayashi, M. Kurosumi, S. Saji, K. Suemasu, T. Okazaki, K. Nakachi, T. Fujita, S. Hayashi, Prediction of prognosis of estrogen receptor-positive breast cancer with combination of selective estrogen-regulated genes, Cancer Sci. 95 (6) (2004) 496-502.

[22] G.J. Herman, R.J. Graff, S. MyöHänen, D.B. Nelkin, B.S. Baylim, Methylation-specific PCR: a novel PCR assay for methylation status of CpG islands, Proc. Natl. Acad. Sci. U.S.A. 93 (18) (1996) 9821-9826.

[23] L.C. Li, R. Dahiya, MethPrimer: designing primers for methylation PCRs, Bioinfomatics 18 (11) (2002) 1427-1431.

[24] M.J. Fasco: Estrogen receptor mRNA splice variants produced from the distal and proximal promoter transcripts, Mol. Cell. Endocrinol. 138 (1998) 51-59.

[25] R.J. Weigel, D.L. Crooks, J.D. Iglehart, E.C. deConinck: Quantitative analysis of the transcriptional start sites of estrogen receptors in breast carcinoma, Cell Growth Differ. 6 (1995) 707-711.

[26] E.C. deConinck, L.A. McPherson, R.J. Weigel: Transcriptional regulation of estrogen receptor in breast carcinomas,
Mol Cell Biol. 15 (1995) 2191-2196

[27] L.A. McPherson, V.R. Baichwal, R.J. Weigel: Identification of ERF-1 as a member of the AP2 transcription factor family. Proc. Natl. Acad. Sci. USA. 94 (1997) 4342-4327.

[28] B.T. Pentecost, R. Song, M. Luo, J.A. DePasquale, M.J. Fasco: Upstream regions of the estrogen receptor alpha proximal promoter transcript regulate ER protein expression through a translational mechanism, Mol. Cell. Endocrinol. 229 (2005) 83-94.

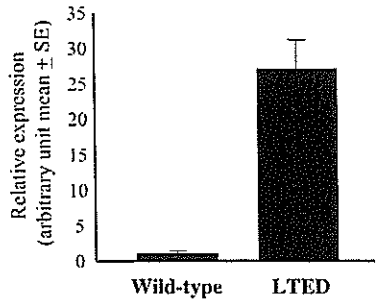

Fig. 1. Relative expression of total ER α mRNA in wild-type and LTED cells. Real-time RT-PCR was conducted for quantification of total ER α and β -actin mRNA as described in Materials and methods. Expression levels of total ER α mRNA were normalized using β -actin mRNA.

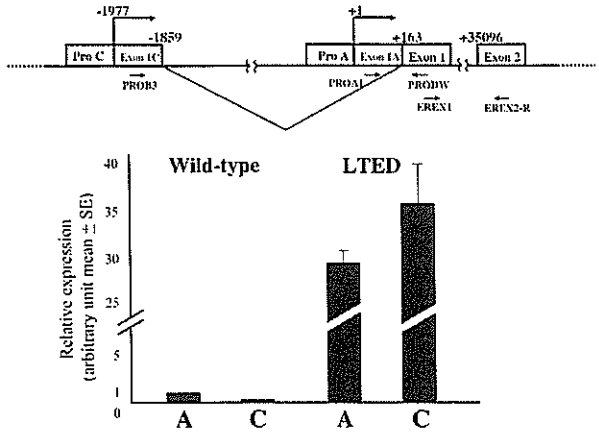

Fig. 2. Expression of ER α mRNA transcribed from promoters A and C in wild-type and LTED cells. Schematic representation of a part of ER α gene organization is shown above. The transcription start site of promoter A is defined as +1. Relative expression of ER α mRNA from promoters A and C in wild-type and LTED cells is shown. Expression levels of ER α mRNA from promoters A and C were quantified by real-time RT-PCR as described in Materials and methods being normalized by β -actin mRNA.

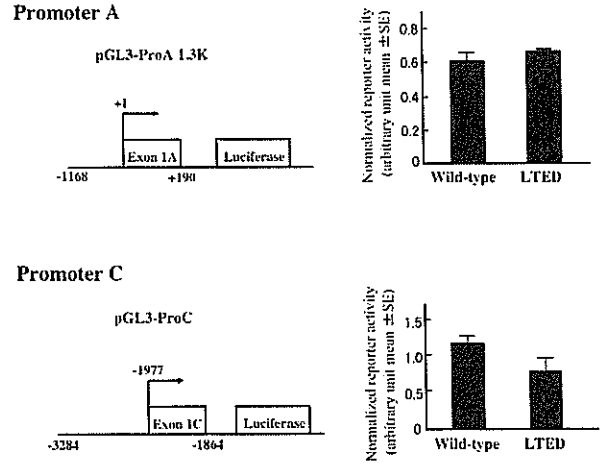

Fig. 3. Reporter activities of promoters A and C in wild-type and LTED cells. Wild-type and LTED cells were transiently transfected with a reporter gene construct pGL3-ProA 1.3K or pGL3-ProC together with control vector pRL-TK as described in Materials and methods. The measured luciferase activities were normalized using the control Renilla luciferase activity.

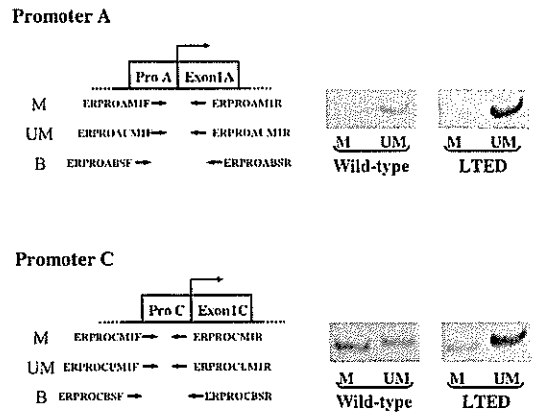

Fig. 4. Methylation-specific PCR analysis of ERα gene promoters A and C in wild-type and LTED cells. Location of primers used in methylation-specific PCR for promoters A and C is shown in the left. Photos of electrophoresis of PCR products of methylated (M) or unmethylated (U) DNA fragments are shown in the right.

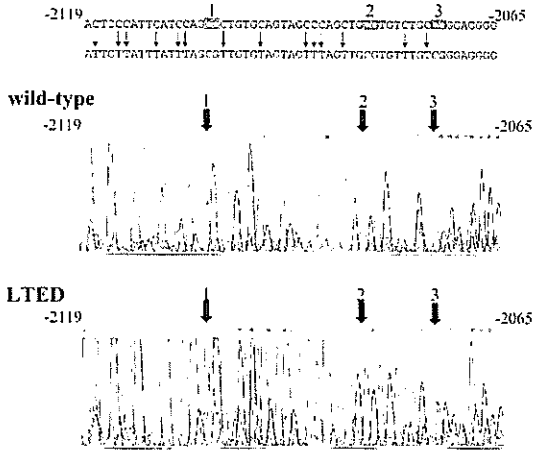

Fig.5. Direct sequencing of PCR products of ER α gene promoter C using bisulfite-converted DNA from wild-type and LTED cells. First PCR products of bisulfite-converted DNA from wild-type or LTED cells using primers ERPROCBSF and ERPROCBSR were subjected to direct sequencing with ERPROCBSF primer as described in Materials and Methods. Three CpG sites within the amplified region are indicated by rectangles with numbering in the upper. Cytosine residues that will be shown as thymine in the sequence of PCR product of bisulfite converted DNA are marked with vertical arrows in black. Thick arrows indicate the positions of three CpG sites.

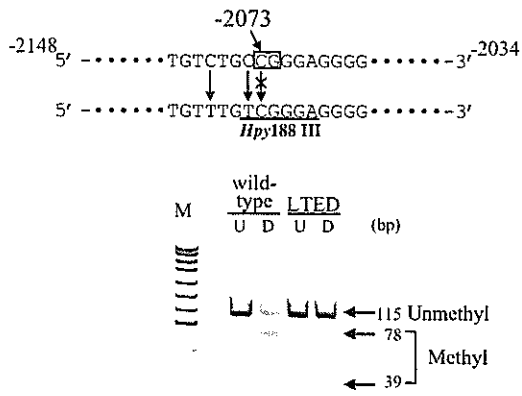

Fig. 6 COBRA assay of ERα gene promoter C in wild-type and LTED cells. First PCR products of bisulfite converted DNA from wild-type or LTED cells using primers ERPROCBSF and ERPROCBSR were digested with restriction enzyme *Hpy*188III as described in Materials and Methods. Rectangle indicates the position of the CpG site to be tested. Underline indicates the recognition site of *Hpy*188III that will be generated by bisulfite conversion of methylated DNA, but not unmethylated one. An image of the polyacrylamide gel electorophoresis is shown below. U, untreated. D, digested with *Hpy*188III.

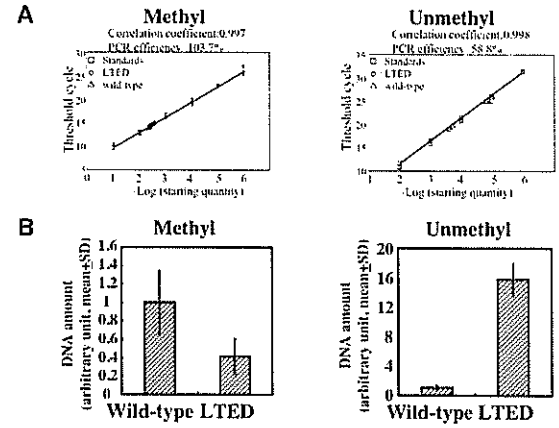

Fig.7 Bisulfite-real-time PCR analysis of ER α gene promoter C in wild-type and LTED cells. Bisulfite-real-time PCR analysis based on SYBR-Green chemistry was conducted using methylation-specific primers ERPROCM1F and ERPROCM1R or unmethylation-specific primers ERPROCUM1F and ERPROCUM1R as described in Materials and Methods. Representative results of bisulfite-real-time PCR are shown above. Comparison of methylated or unmethylated DNA amounts in tested samples from wild-type and LTED cells are shown below. SD, standard deviation.

MOLECULAR CARCINOGENESIS 46:242–248 (2007)

The Presence of *BRAF* Point Mutation in Adult Papillary Thyroid Carcinomas From Atomic Bomb Survivors Correlates With Radiation Dose

Keiko Takahashi,[1,5] Hidetaka Eguchi,[1] Koji Arihiro,[6] Reiko Ito,[1] Kojiro Koyama,[2,8] Midori Soda,[3] John Cologne,[4] Yuzo Hayashi,[7] Yoshihiro Nakata,[5] Kei Nakachi,[1] and Kiyohiro Hamatani[1]*

[1]*Department of Radiobiology/Molecular Epidemiology, Radiation Effects Research Foundation, Hiroshima, Japan*
[2]*Department of Epidemiology (Hiroshima), Radiation Effects Research Foundation, Hiroshima, Japan*
[3]*Department of Epidemiology (Nagasaki), Radiation Effects Research Foundation, Nagasaki, Japan*
[4]*Department of Statistics, Radiation Effects Research Foundation, Hiroshima, Japan*
[5]*Department of Pharmacology, Hiroshima University Graduate School of Biomedical Sciences, Hiroshima, Japan*
[6]*Department of Pathology, Hiroshima University Medical Hospital, Hiroshima, Japan*
[7]*Department of Pathology, Hiroshima Asa Citizen's Hospital, Hiroshima, Japan*
[8]*Department of Urology, Oumu Municipal National Health Insurance Hospital, Hokkaido, Japan*

In papillary thyroid carcinogenesis, the constitutively activated mitogen-activated protein (MAP) kinase signaling pathway caused by a genetic alteration such as *RET/PTC* rearrangement or mutation of *RAS* and *BRAF* genes, is thought to be a major early event. Among these, the recently identified $BRAF^{V600E}$ mutation has been found at high frequency in adult patients with papillary thyroid carcinoma (PTC). However, the association between this mutation and radiation exposure in adult PTC is still unknown. In this study, we examined the $BRAF^{V600E}$ mutation in 64 PTCs among adult atomic bomb survivors in Hiroshima, Japan, comprising 17 nonexposed (0 mGy) and 47 exposed patients who developed the carcinoma after the bombing, and assessed the association of $BRAF^{V600E}$ mutation with clinicopathological and epidemiological variables. The median radiation dose in PTCs with the $BRAF^{V600E}$ mutation was significantly lower than that without the mutation (18.5 vs.156.9 mGy, Wilcoxon rank-sum test, $P=0.022$). A significant difference was found in the median latency period (years elapsed from atomic bombing to diagnosis) between exposed patients with and without $BRAF^{V600E}$ mutation (29 vs. 21 yr, Wilcoxon rank-sum test, $P=0.014$). These findings were further confirmed by logistic regression analysis with $BRAF^{V600E}$ mutation status as a dependent variable and taking into account possible interactions between the variables. We found that the log-transformed radiation dose and latency period were independently associated with the $BRAF^{V600E}$ mutation ($P=0.039$ and $P=0.010$, respectively). These results suggest that involvement of *BRAF* mutation in thyroid carcinogenesis in exposed people may differ from that in the nonexposed people.

Key words: $BRAF^{V600E}$ mutation; radiation dose; latency period; thyroid carcinogenesis

INTRODUCTION

Thyroid cancer is well-known to be associated with exposure to external or internal ionizing radiation, such as from the atomic bomb (A-bomb) or the Chernobyl accident. The excess relative risk of thyroid cancer per Sv was 1.15 in the Life Span Study of A-bomb survivors [1], and a strong relationship between thyroid cancer and radiation dose was indicated from the Chernobyl accident [2].

In papillary thyroid carcinogenesis, constitutive activation of the MAP kinase signaling pathway caused by a genetic alteration, including rearrangements of *RET/PTC* or mutation of *RAS* and *BRAF* genes, is thought to be a major early event [3–5]. Among these alterations, the *BRAF* gene mutation in the pathogenesis of papillary thyroid carcinoma (PTC) has recently gained considerable attention.

The *BRAF* gene encodes a serine/threonine kinase responsible for the transduction of signals in the MAP kinase cascade, which leads to the regulation of transcription factors, cytoskeletal elements, and other protein kinases that control cell proliferation [6]. *BRAF* somatic mutations were first discovered in several types of human cancers, including malignant melanomas, and colorectal and ovarian cancers [7].

Abbreviations: MAP kinase, mitogen-activated protein kinase; PTC, papillary thyroid carcinoma; A-bomb, atomic bomb; mGy, milli gray.

*Correspondence to: Department of Radiobiology/Molecular Epidemiology, Radiation Effects Research Foundation, 5-2, Hijiyama-Park, Minami-ku, Hiroshima, 732-0815, Japan.

Received 28 April 2006; Revised 9 August 2006; Accepted 9 August 2006
DOI 10.1002/mc.20277

Except for very rare instances, the *BRAF* mutation identified in thyroid cancer so far is almost exclusively the thymine-to-adenine transversion at nucleotide 1799, resulting in the substitution of glutamate for valine at residue 600 (V600E) [8]. The V600E (formerly called V599E) substitution is thought to convert BRAF inactive conformation into its active form by disrupting the residue–residue interaction between the activation loop and the ATP binding site [9]. Recent data on the frequent prevalence of $BRAF^{V600E}$ mutation in thyroid microcarcinomas support the hypothesis that $BRAF^{V600E}$ mutation is an early event in PTC pathogenesis [10], along with the induction of goiter or invasive PTC in $BRAF^{V600E}$ transgenic mice [11].

$BRAF^{V600E}$ mutation has so far been described as occurring with a frequency ranging from 29 to 83% in PTC from adult patients [8]. In order to clarify the role of the $BRAF^{V600E}$ mutation in PTC, associations of the $BRAF^{V600E}$ mutation and clinico-pathological and epidemiological factors in PTC have been examined [8]. Among the common subtypes of PTC, prevalence of the $BRAF^{V600E}$ mutation showed a clear association with histological subtype. The highest frequency was in tall cell PTC (overall 77%), the second highest in conventional PTC (overall 60%), and the lowest in follicular variant PTC (overall 12%) [8], implying the possible role of $BRAF^{V600E}$ mutation in the determination of histology of PTC. The relationship between $BRAF^{V600E}$ mutation frequency and age at diagnosis in adult patients is still controversial. Both a significant correlation [12,13] and no correlation [14–17] have been reported. Thus, presence or absence of $BRAF^{V600E}$ mutation may be a key event for characterization of PTC, as is the case in colon cancer [18].

With regard to the relation to radiation exposure, the $BRAF^{V600E}$ gene mutation was studied in a type of radiation-related PTC, postChernobyl PTC, which is believed to have developed in those exposed to radiation as children. Very low frequencies of $BRAF^{V600E}$ mutation in this PTC have been reported (range: 0–12%) [19–23]. However, the prevalence of $BRAF^{V600E}$ mutation was also low (range: 0–6%) in PTC among children and adolescents who were not exposed to radiation [19,20,23]. A low prevalence of the $BRAF^{V600E}$ mutation has thus been observed in childhood PTC regardless of the presence or absence of past radiation exposure.

On the other hand, the association of the $BRAF^{V600E}$ mutation with radiation exposure has not been studied in adult PTC with history of radiation exposure. Because the prevalence of $BRAF^{V600E}$ mutation has been reported to be high in adult PTC [8], analysis of the association of $BRAF^{V600E}$ mutation with radiation exposure in adult PTCs is particularly important.

In this study, we compared clinico-pathological and epidemiological characteristics of adult PTC among A-bomb survivor patients by $BRAF^{V600E}$ mutation status.

MATERIALS AND METHODS

Tissue Specimens

Study subjects comprised 64 cases of adult PTC found among A-bomb survivors in Hiroshima. Classification of histology was done according to histopathological typing of the World Health Organization [24]. Study materials were formalin-fixed and paraffin-embedded thyroid tissue specimens obtained from the subjects between 2003 and 2005 under approval of the Human Investigation Committee and the Ethics Committee for Genome Research at the Radiation Effects Research Foundation (RERF).

DNA Preparation and Determination of $BRAF^{V600E}$ Mutation

Five-micrometer tissue sections were deparaffinized, stained with Methyl Green (Sigma-Aldrich, St. Louis, MO) and dissected manually or using laser microdissection system Leica AS LMD (Leica, Wetzler, Germany). DNA was extracted from the microdissected noncancerous or cancerous regions using QIAamp DNA Micro kit (QIAGEN, Hilden, Germany). Polymerase chain reaction (PCR) was performed in a 25 μL mixture containing 10 pmoles of each primer, 200 μM of each dNTP, 0.5 U of FastStart High Fidelity DNA polymerase (Roche, Basel, Switzerland), 20–50 ng of genomic DNA, and 1× reaction buffer supplied by the manufacturer. PCR conditions consisted of initial denaturation (95°C for 2 min), followed by 40 cycles (denaturation at 94°C for 30 s, annealing at 54°C for 60 s, extension at 72°C for 30 s). Primers used were 5′-tcatgaagacctcacagtaaaaat-3′ and 5′-tggatccagacaactgttcaa-3′. $BRAF^{V600E}$ mutation was initially screened by restriction fragment length polymorphism (RFLP) using restriction enzyme *Tsp*RI (New England Biolabs, Ipswich, MA) and was confirmed by direct sequencing using DNA sequencer CEQ8000 (Beckman Coulter, Inc., Fullerton, CA).

Statistical Analysis

Univariate analysis for comparison of clinico-pathological and epidemiological variables by radiation exposure or $BRAF^{V600E}$ mutation status was conducted using nonparametric tests (Wilcoxon rank-sum test) for continuous variables, because the distribution of radiation dose and latency period could not be assumed to be symmetrical. Fisher's exact was used for categorical variables. Logistic regression analysis was carried out among A-bomb survivor patients who were exposed to atomic

radiation, and we assessed the relationship between $BRAF^{V600E}$ mutation status and clinico-pathological and epidemiological variables including log- transformed radiation dose, latency period, histology, gender, and age at the time of A-bombing (or age at diagnosis). All statistical analyses were performed with SPSS software (version 12.0).

Radiation Dose

A-bomb radiation doses used in this analysis were estimated by the recently implemented DS02 system [25].

RESULTS

Noting that almost all PTC in A-bomb survivor patients occurred in adults, we examined the $BRAF^{V600E}$ mutation in 64 adult PTC cases among A-bomb survivor patients (cohort members of the Life Span Study) in Hiroshima, Japan, comprising 17 nonexposed (0 mGy) and 47 exposed patients (median dose: 150.7 mGy) who developed carcinoma after the bombing. All thyroid cancer tissue samples used were formalin-fixed, paraffin-embedded surgical specimens resected during 1956–1993. Patient characteristics such as gender, age at the time of A-bombing, age at diagnosis, latency period (years from A-bombing to diagnosis, being defined only for exposed patients), and histological subtypes are summarized in Table 1. All patients analyzed in this study were diagnosed at the age of 20 yr or older. All tumors were well-differentiated PTC including three cases of follicular variant; none was a solid variant.

DNA samples were extracted from microdissected specimens of cancerous or noncancerous tissue. We first conducted screening of $BRAF^{V600E}$ mutation by RFLP, followed by direct sequencing of the fragments to confirm the mutation (Figure 1). The frequency of $BRAF^{V600E}$ mutation in nonexposed patients (71%) was in good agreement with that reported for conventional adult PTC (Table 1) [8].

We then examined whether $BRAF^{V600E}$ mutation status in PTC in all A-bomb survivor patients consisting of both the nonexposed and the exposed people is related to any clinico-pathological or epidemiological characteristics, including radiation dose, age at the time of A-bombing, and age at diagnosis. The relationship between $BRAF^{V600E}$ mutation status and each factor is summarized in Table 2. The median radiation dose in PTC with $BRAF^{V600E}$ mutation was significantly lower than that in PTC without $BRAF^{V600E}$ mutation (Table 2, $P = 0.022$). Furthermore, a marginally significant association was found between $BRAF^{V600E}$ mutation status and histological subtype (Table 2, $P = 0.062$); all three cases of follicular variant harbored wild-type *BRAF*. This was in agreement with the previous observation of a low prevalence (12%) of $BRAF^{V600E}$ mutation in follicular variant PTC [8]. On the other hand, age at the time of A-bombing, age at diagnosis, and gender did not evidence significant association with $BRAF^{V600E}$ mutation status in the univariate analysis.

Additionally, an analysis on clinico-pathological or epidemiological characteristics including latency period that can be defined only for exposed patients was also undertaken in relation to $BRAF^{V600E}$ mutation with only the 47 exposed patients (Table 2). In addition to the characteristics found to be associated with $BRAF^{V600E}$ mutation status in all patients,

Table 1. Clinico-Pathological and Epidemiological Characteristics of Patients by Radiation Exposure Status

	Nonexposed patients[a] ($n = 17$)	Exposed patients ($n = 47$)	*P*-value
$BRAF^{V600E}$ mutation			
Present (*n*)	12	26	0.4[c]
Absent (*n*)	5	21	
Frequency (%)	71	55	
Median radiation dose (mGy, range)	0	150.7 (0.4–2758)	
Median latency period[b] (yr, range)	—	26.0 (11–46)	
Median age at the time of atomic-bombing (yr, range)	21.0 (5–52)	25.0 (1–49)	0.4[d]
Median age at diagnosis (yr, range)	48.0 (34–84)	54.0 (20–89)	0.6[d]
Histology			
Conventional PTC (*n*)	17	44	0.6[c]
Follicular variant (*n*)	0	3	
Gender			
Male (*n*)	1	5	1.0[c]
Female (*n*)	16	42	

[a]The nonexposed patients were either those with radiation dose estimated to be 0 mGy or those who were not in the city of Hiroshima at the time of bombing.
[b]Latency period: years from A-bombing to diagnosis.
[c]Fisher's exact test.
[d]Wilcoxon rank-sum test.

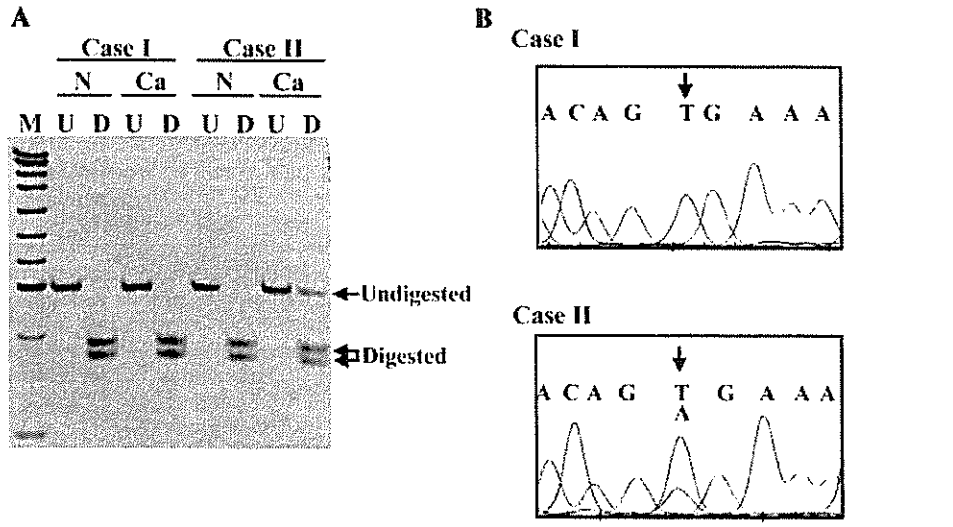

Figure 1. Detection of *BRAF*^{V600E} mutation. (A) RFLP analysis of *BRAF*^{V600E} mutation. DNA fragments containing nucleotide position 1799 were amplified and subsequently digested with restriction enzyme *Tsp*RI, as described in Materials and Methods. Representative results of gel electrophoresis of two samples are shown. N indicates noncancer; Ca, cancer; U and D, undigested and digested with *Tsp*RI; and M, molecular weight marker, respectively. Horizontal arrows indicate positions of undigested- or digested-bands. *Tsp*RI digests wild-type fragments, but not mutated ones. (B) Direct sequencing of PCR fragments. Sequences of the fragments amplified using DNA from tissue specimens of cases I and II are shown. Vertical arrow indicates nucleotide positions 1799. Heterozygous signal of T and A was detected for case II.

latency period also showed a statistically significant association with the mutation; the median latency period in PTC with *BRAF*^{V600E} mutation was significantly longer than that in PTC without the mutation (Table 2, $P=0.014$).

Because these clinico-pathological and epidemiological variables may be interrelated, we further performed multivariate logistic regression analysis for the 47 exposed patients, with *BRAF*^{V600E} mutation status as the dependent variable (Table 3). Log-transformed radiation dose was used as an explanatory variable, because the distribution of log-transformed radiation dose could be assumed to be nearly symmetrical, whereas that of nontransformed radiation dose could not. Log-transformed radiation dose showed a significant inverse association with *BRAF*^{V600E} mutation ($P=0.039$), and latency period revealed a significant positive association ($P=0.010$), confirming the results of univariate analyses shown above. The same result was obtained when age at the time of A-bombing was substituted for age at diagnosis as a variable in the regression analysis.

DISCUSSION

In papillary thyroid carcinogenesis, constitutive activation of the MAP kinase signaling pathway, namely *RET* and *NTRK* tyrosine kinase receptor rearrangements and *RAS* and *BRAF* oncogene activation, seems to be required for transformation [26]. Interestingly, mutual exclusion of these genetic events in the MAP kinase signaling pathway was reported between *BRAF* mutation and *RET/PTC* rearrangements, and between *BRAF* and *RAS* mutations [3–5,21,27–30]. Furthermore, a recently identified *AKAP9-BRAF* rearrangement was not shared with *BRAF* mutation in radiation-associated PTC [22]. Thus, no PTC case possessed more than one of the following mutational events: *BRAF*^{V600E}, *NTRK1* or *RET/PTC* rearrangements [5]. These data suggest that a single genetic event in the MAP kinase signaling pathway may be sufficient for thyroid cell transformation and tumorigenesis. Recent in vitro and in vivo experiments have also demonstrated the requirement of activation of the RET/PTC-RAS-BRAF-MAPK pathway in thyroid tumorigenesis [34–36].

In our study, we found that 71% (12/17) of PTC among nonexposed PTC patients had *BRAF*^{V600E} mutation, indicating that among the several events in the RET/PTC-RAS-BRAF-MAPK pathway, *BRAF*^{V600E} mutation is the most common for non-exposed adult Japanese PTC patients. On the other hand, *BRAF*^{V600E} mutation accounted for only 17% (2/12) of the adult PTC patients who were exposed to radiation dose greater than 500 mGy. These findings suggest that *BRAF*^{V600E} mutation is not a major event in the development of radiation-associated PTCs in adult patients, such as A-bomb survivors with high radiation exposure.

On the other hand, *RET/PTC* rearrangements have been shown to be particularly prevalent in PTCs from